

Creep effects in nanoindentation of hydrated phases of cement pastes

Jiří Němeček*

Czech Technical University in Prague, Faculty of Civil Engineering, Department of Mechanics, Thákurova 7, 16629 Prague 6, Czech Republic

ARTICLE DATA

Article history:

Received 23 August 2007

Received in revised form 9 June 2008

Accepted 9 April 2009

Keywords:

Nanoindentation

Micromechanical properties

Cement paste

Creep

Size effect

ABSTRACT

This paper focuses on the nanoindentation of cement pastes and their micromechanical response. Since cement paste is a heterogeneous material at microscale, micromechanical properties have to be assessed separately for its individual material phases, i.e. hydrated products and unhydrated phases. Our study addresses important issues concerning experimental loading paths and their effects on the evaluation of elastic properties using nanoindentation. The effect of creep is shown on a series of multicycle experiments. A wide range of maximum loads and corresponding final penetration depths (approximately 200–1200 nm) are covered in this study. Experimental measurements on both hydrated cement samples and on unhydrated clinker minerals have proved that significant creep deformation can be attributed purely to hydrated phases. Further, it has been found that cement paste exhibits a strong size effect on elastic properties measured by nanoindentation and evaluated by the standard Oliver–Pharr procedure for loading–unloading tests with no dwell period at the peak load. Such property was already reported for plastic materials like metals [Elmustafa AA., Stone DS., Indentation size effect in polycrystalline F.C.C. metals, *Acta Materialia* 2002; 50 (14): 3641–3650., Wei, Y., Wang, X., Zhao, M., Size effect measurement and characterization in nanoindentation test, *Journal of Material Research* 2004; 19 (1): 208–217.], due to various effects but creep. As shown in the paper, cyclic loading and using long dwell periods at peak load leads to minimizing of this spurious type of size effect. Moreover, comparison with results obtained for the COC/PE polymer (75% cycloolefin copolymer + 25% polyethylene) has been performed. This polymer has been found to exhibit similar time-dependent behavior as hydrated cement paste.

© 2009 Elsevier Inc. All rights reserved.

1. Introduction

The development of various experimental techniques in the past decades has made possible the assessment of mechanical properties of various materials and their constituents at submicron length scales. Nanoindentation plays an important role among these experimental techniques. It is based on the direct measurement of the load–displacement relationship using a very small tip (usually diamond) pressed into the material. Although nanoindentation was originally developed and used mainly for studying homogeneous materials like

metals, coatings, films, glass and crystal materials, the evolution of this method allows us to use it also for cementitious materials. Major studies can be found e.g. in [3,4,15]. However, the interpretation of measured data is more complicated due to the large heterogeneity of cement.

It is also a well-known fact that, in contrary to classical macroscopic tests, numerous microscale phenomena can occur during indentation tests. Size-dependent indentation results are commonly obtained and reported mainly for metals by many researchers, e.g. in [2,7,16]. This size effect found in the literature concerns mainly hardness as the only

* Tel.: +420 2 2435 4309; fax: +420 2 2431 0775.

E-mail address: jiri.nemeczek@fsv.cvut.cz.

parameter characterizing load-depth diagrams obtained from indentation tests. As will be shown in the paper, a similar size effect can be found for elastic modulus in the case of cementitious material. Creeping of hydrated phases of this material was found to be the main factor contributing to such interpretations. Ignoring creep and other inelastic phenomena can lead to the spurious size effect on elastic properties and their overestimation.

2. Nanoindentation of Cement Pastes

Several methods for interpreting nanoindentation results have been proposed in the past. Some of the favorite methods are those authored by Oliver and Pharr [14] or Doerner and Nix [6]. These methods for the assessment of elastic properties are generally based on the assumption of indentation in a homogeneous body. In contrary, the cementitious matrix is a heterogeneous material containing very distinct phases on the micrometer scale. These are mainly hydration products (C-S-H gels, Portlandite and other minor constituents), unhydrated grains of clinker minerals and porosity. Hydrated phases occupy the majority of the specimen volume and they are of prior importance for the overall material response. Therefore, results from nanoindentation of the cementitious matrix have to be separated and evaluated for its individual constituents. In this paper, only results for hydrated phases have been taken into account from the nanoindentation of cement paste samples. Indents produced to unhydrated clinkers have not been considered because their properties are affected by the embedment in the surrounding hydrated matrix. Clinker properties have been assessed on samples of pure non-hydrated cement clinker. All elastic properties in this study have been computed according to the Oliver–Pharr [14] methodology.

3. Indentation Size Effect

The effect of the structural size on its strength is widely known and can be understood as the effect of the structural dimension on the nominal strength of the structure when geometrically similar structures are compared. Such sizing is caused mainly by inelastic phenomena that take place in different structural volumes and result in different strengths. In the case of elastic properties, one would expect constant values for a homogeneous isotropic material regardless of the sample size or the size of an indent. A variety of reasons are responsible for a more complicated material behavior and the interpretation of experimental data on the microscale. The most important are summarized below.

1. Specimen preparation. Samples must often undergo a series of mechanical procedures to obtain a flat and smooth surface suitable for indentation. These procedures such as grinding and polishing can produce residual stresses within the surface layers of the material and cause local hardening.

2. Oxidation. Thin oxide layers with mechanical properties different from bulk properties can distort measurements on materials sensitive to oxidation.
3. Indenter friction and adhesion. Some studies also show the effects of friction [12] and adhesion forces [9] between the indenter tip and a sample. Such effects may be significant for soft materials but mainly for small penetration depths (typically less than 100 nm).
4. Surface roughness. Evaluation procedures assume a flat surface with the ideal contact of an indenter. High surface roughness can lead to improper area determination and/or higher local inelastic deformations.
5. Indenter area function. A common source of the indentation size effect is improper estimation of the projected indenter area. Each indenter has to be calibrated due to tip irregularities from its ideal shape. An effective procedure for such calibration was proposed in [14].
6. Development of dislocations. Another reason based on the indentation process can be responsible for the size effect. It is the nucleation of dislocations within the plastic zone under the indentation area [8,13]. Dislocations can be created in two ways: for statistical reasons and due to the indenter geometry (geometrically necessary dislocations). The presence of dislocations increase the yield strength of the material and this in turn increases the hardness and elastic modulus.
7. Loading time effects. The time of loading (and also unloading) is usually not considered in the evaluation of elastic properties. However, as will be shown later, time-dependent material properties can influence the loading diagram from which elastic properties are extracted. Generally speaking, such phenomena associated with loading time (that are called creep below for simplification) are responsible for misinterpretation when using standard tests and standard evaluation procedures.

3.1. Discussion on the Sources of the Indentation Size Effect

The aforementioned items 1 to 3 are significant for small indents (less than 100 nm) where the depth of penetration affects only the surface layers. For our case, the smallest indentation depth was around 200 nm and the majority of experiments were conducted on larger scales where the affected material volume is considerably larger. Surface roughness cannot be fully avoided for cementitious materials since the mechanical preparation of the surface does not allow preparing better surfaces with roughnesses smaller than several tens of nm (as checked by AFM). However, a large number of indents allow statistical evaluation of results, where such local effects are minimized (indicated by standard deviations). The assessment of the indenter area function can be effectively solved using the Oliver–Pharr [14] procedure. This procedure was also employed in our case. Moreover, the depth of indents was large enough to avoid these problems that are present for indents having dimensions close to the indenter tip. The development of dislocations is inevitably present but again it is more significant for small indents and plastic like materials (e.g. metals). Creep effects are very important for soft and time-dependent materials like cement paste. It will be shown in the results that loading and dwelling

time is the main factor causing the spurious size effect on the evaluation of elastic properties.

4. Experimental Part

4.1. Cement Paste Samples

All samples were made of white cement CEM-I 52,5 White (Holcim, SK). Cement was mixed with water in the water/cement ratio $w/c=0.5$ by weight. The mixture was placed in small plastic cylindrical moulds with the volume of 31 cm^3 and vibrated immediately after casting to remove entrapped air. After that, specimens were cured in water for 2 months. Before testing, a 2 mm thick slice of a specimen was cut at the middle third of the cylinder. Before nanoindentation, the surface was prepared by mechanical grinding and polishing on coarse to very fine emery papers to achieve a very smooth and flat surface [5]. Specimens were subsequently washed in ultrasonic bath to remove all dust particles and dried. The resultant surface had the roughness of about several tens of nm at the place on indentation as checked by the atomic force microscope (AFM). A typical value of the parameter root-mean-square (RMS), defined according to [11] as follows:

$$\text{RMS} = \sqrt{\frac{1}{A \cdot B} \sum_{i=1}^A \sum_{j=1}^B h_{ij}^2}$$

was 20–50 nm (evaluated over the whole indentation area). In this formula, h_{ij} has the meaning of the surface height measured at the position i, j whose number is A and B , respectively.

4.2. Samples of Cement Clinker

In order to distinguish between the time-dependent behavior of hydrated cement phases and clinker minerals separate samples of dry polished clinker were prepared. The grain of industrial cement clinker taken at the cement works was first imbedded in dentacryl poured to the cylindrical mould. Then it was cut in the middle and the surface was dry polished to achieve a roughness less than 50 nm. Industrial cement clinker is a compound of different natural minerals. There are two major constituents called alite and belite. They are related to pure chemical phases-tricalcium silicate (C_3S) and dicalcium silicate (C_2S). Further, tricalcium aluminate (C_3A) and calcium aluminoferrite (C_4AF) can be present in clinker. Our sample was taken directly from the cement works and thus it consisted of a mix of these phases. Using the EDX analysis in ESEM it was determined that the places used for subsequent indentation were created mainly by belite (C_2S) and, therefore, results were computed for this phase.

4.3. Samples of COC/PE

For comparison purposes, samples of another material were tested. The COC/PE polymer (75% cycloolefin copolymer + 25% polyethylene) was chosen due to its high ductility and similar creeping behavior compared to cement paste at the micro-scale. The COC/PE polymer is commonly used for implants in

biomechanical engineering. Small cuts of COC/PE were prepared in a similar way, i.e. polished on fine emery papers and diamond pastes to achieve $\text{RMS} < 50 \text{ nm}$.

4.4. Methods

First, the cement paste sample was scanned in optical and electron microscopes (XL30 ESEM-TMP, Philips Ltd.) to select a suitable place for indentation with a minimum roughness and a large amount of well-hydrated phases. The surface roughness of the selected place was scanned by AFM to check that the parameter RMS is less than 50 nm. The place with well-hydrated cement and a small amount of unhydrated material was selected in order to produce the majority of indents to hydrated phases. Indents lying in unhydrated phases had to be subsequently excluded from considerations. Generally, cementitious materials exhibit a much larger scatter of material properties compared to metals or similar homogeneous materials. To overcome this difficulty it is necessary to produce a large number of indents into the same material constituent and perform statistical evaluation of the results. In our case, a matrix of at least 70 indents covering a large region of the material was selected (Fig. 1). The distance

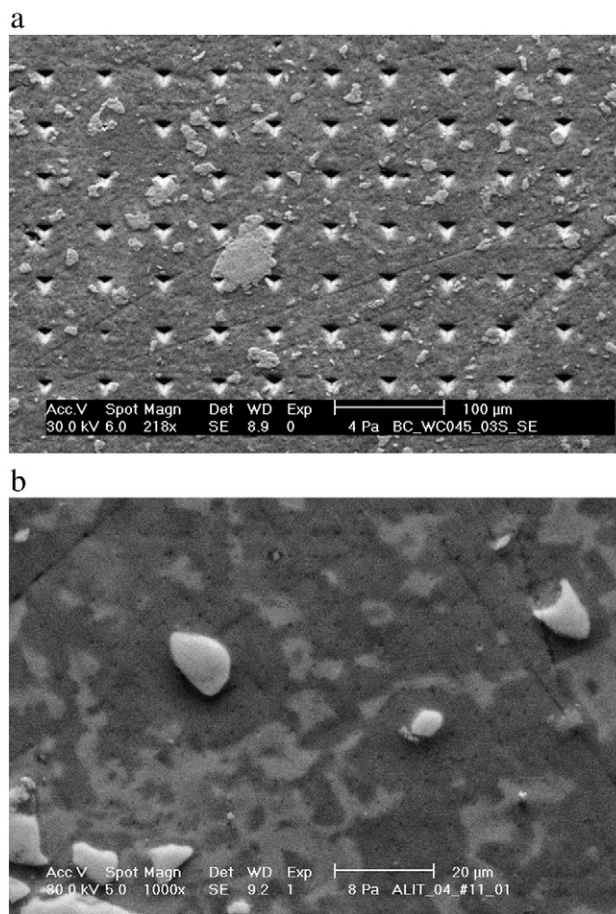


Fig. 1 – The microstructure of cement paste taken in ESEM. (a) A large indentation matrix performed to the maximum applied load. (b) Small indents (hardly visible black dots) performed to the minimum load.

between individual indents was set at least ten times of their final depth (approximately 5–50 μm) to avoid a mutual influence. For all measurements the Nanotest nanoindenter (by Micro Materials, UK) equipped with a standard Berkowich tip was used. After the indentation all individual indents were scanned again in the electron microscope and only those fully lying in hydrated cement were considered in the evaluation. The separation of phases was based on 2-D imaging in ESEM but also on the X-ray element analysis (EDX) in the electron microscope.

Two kinds of experiments were performed. For the first series (marked “O”), multiple loading cycles to increasing loads were used. Each indent consisted of 8 cycles to increasing peak loads of 2–20 mN. This load range corresponds to the final depth range of approximately 200–1200 nm. Unloading to 30% of the peak load was performed before the next indentation cycle. No dwell period at the peak was used in this case. This loading path is shown in Fig. 2a. The time course of a single cycle is shown in Fig. 3. Loading was prescribed with a constant strain rate $\dot{\epsilon} = \frac{1}{2} \frac{P}{P} = 0.15 \text{ s}^{-1}$. Linear unloading lasted for 45 s for all cycles.

For the second series (marked “C”), five loading/unloading cycles to the same load level were performed (Fig. 2b). Again, several load levels (2, 4, 8, 15, 20 mN) were chosen to cover large range of penetration depths. The time course of loading was the same like for “O” series with the dwell period at the peak in addition (Fig. 3). The dwell period was

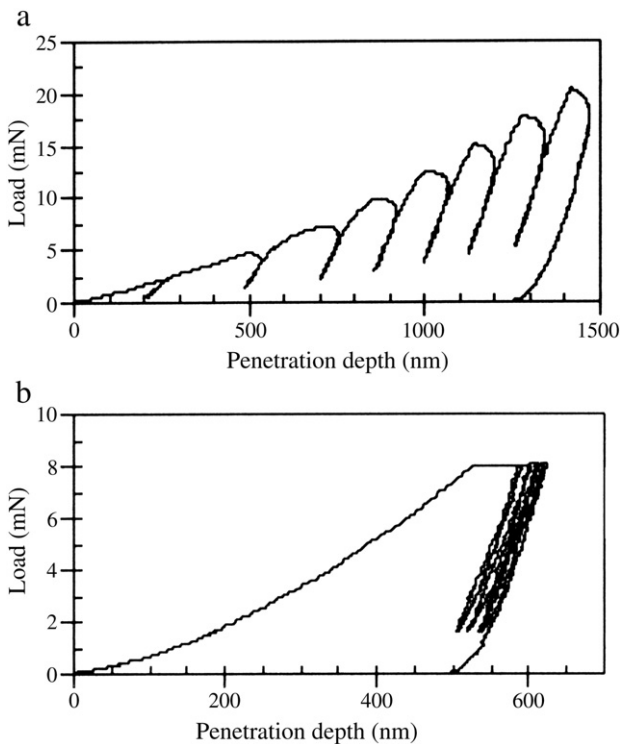


Fig. 2 – Examples of loading diagrams. (a) Series “O”—multiple loading cycles with increasing load 2–20 mN with no dwell period at peaks. (b) Series “C”—5 loading/unloading cycles to the same load (8 mN) with a dwell period at the peak of 120 s.

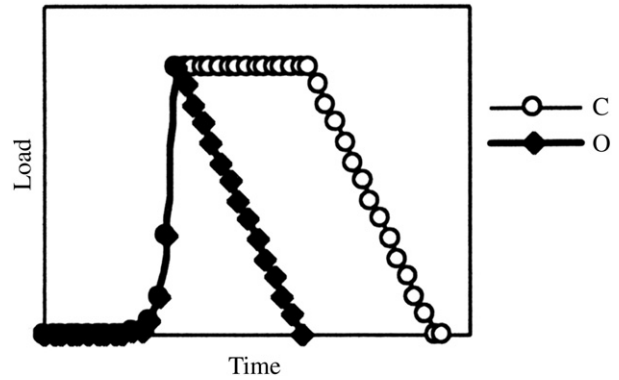


Fig. 3 – Time course of a single cycle: exponential loading to the peak, dwell period (only “C” series) and linear unloading.

chosen as relatively long, 120 s, to allow creeping (Figs. 2b and 4). It can be seen in Fig. 4 that a significant amount of creep deformation is present in the first loading cycle. The successive cycles contain a very small amount of deformation increase compared to the absolute value of the first cycle deformation (less than 5%).

The measurement of COC/PE was carried out in a similar manner. Multiple loading cycles to increasing loads with no dwell period at the peak (series “O”) as well as cyclic loading to the same load with a dwell period at the peak (series “C”) were performed.

5. Results

5.1. Evaluation of Measurements

Micromechanical properties were evaluated according to the Oliver–Pharr [14] methodology. Two elastic properties can be derived from the unloading part of the load-depth diagram.

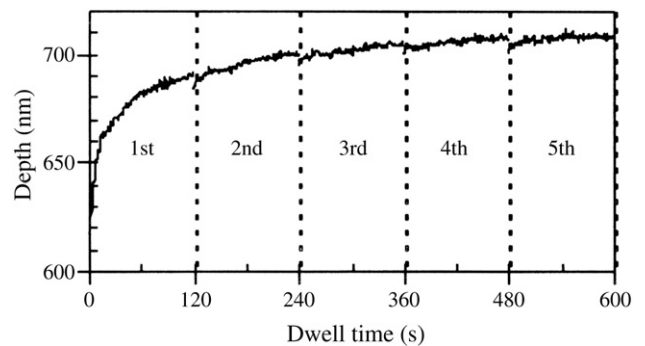


Fig. 4 – Example of the depth increase (creep deformation) during five dwell periods at cycle peaks (series “C”) for the load level of 8 mN. Each column corresponds to one 120 s long cycle. Note that loading and unloading is present between dwell periods (Fig. 1b).

The hardness H and the indentation modulus M are defined as follows:

$$H = \frac{P_{\max}}{A} \quad (1)$$

$$M = \frac{S\sqrt{\pi}}{2\sqrt{A}}, \quad (2)$$

where P_{\max} is the peak load, A is the projected contact area at peak load and S is the contact stiffness evaluated as the initial slope of the unloading curve. Elastic modulus can be derived from indentation modulus using the following equation accounting for the effect of a non-rigid indenter and the substrate as:

$$\frac{1}{M} = \frac{1-\nu^2}{E} + \frac{1-\nu_i^2}{E_i}, \quad (3)$$

where E and ν are the elastic modulus of the tested material and Poisson's ratio, respectively. E_i and ν_i are indenter's parameters (for diamond: $E_i=1141$ GPa and $\nu_i=0.07$).

The peak value of the deformation during the dwell period is increasing for creeping material like cement paste (Fig. 4). Therefore, the evaluation of hardness is ambiguous due to the evolution of the contact area during this period. As the deformation and contact area are increasing during the dwell period the related hardness is decreasing. Creep is also inevitably present on the loading branch of the diagram. Different loading times and different load levels yield different hardness values as for the creeping material. Therefore, hardness is not a suitable parameter for comparisons and only indentation modulus is used in subsequent considerations.

5.2. Cement Paste

As the result of measurements the indentation modulus M was evaluated for each indent lying in the hydrated phase of cement paste and for each loading cycle. Statistical evaluation of elastic properties was applied for selected indents of the same material phase (at least 70 indents). Mean values of M with standard deviations are shown in Fig. 5 for both series. A

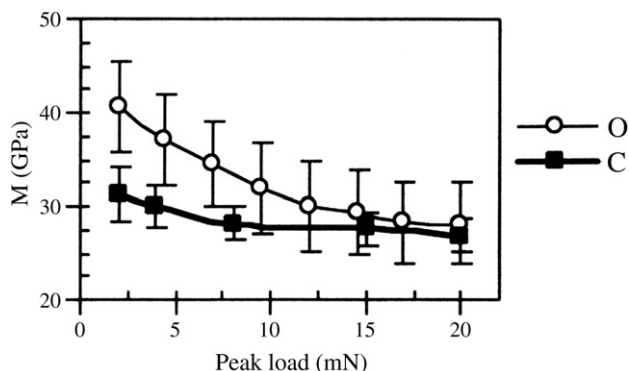


Fig. 5 – Indentation modulus evaluated for hydrated phases of cement paste. The thin lines represent results for “O” series with increasing loading cycles without a dwell period at the peak, whereas the thick lines stand for “C” series tested by cyclic loading to the same load with a 120 s dwell period at the peak.

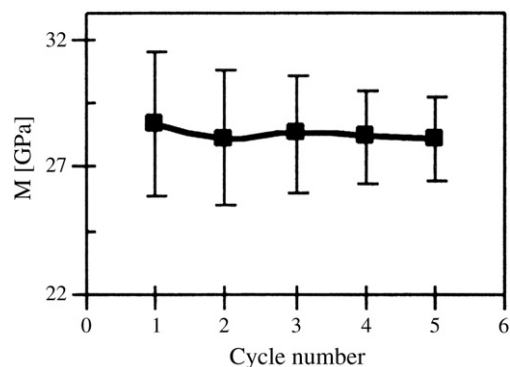


Fig. 6 – Indentation modulus evaluated from 5 cycles measured on “C” samples (peak load 8 mN).

relatively large scatter of results in some cases can be attributed to the heterogeneity of the sample over the indentation area. It can be seen from Fig. 5 that for “O” series the indentation modulus M decreases as the peak load increases. This significant size effect on M is caused by the influence of creep which is present at the beginning of the unloading branch. This creep is indicated by the “rounding” of the upper part of the unloading curve in each cycle (Fig. 2a).

In contrast, this spurious size effect on M is significantly reduced using a long dwell period at peak load as for “C” series. Moreover, cycling to the same peak load was applied to discover creep increments in subsequent cycles. It has been found that the majority of the entire creep deformation takes place in the first cycle as shown in Fig. 4. Increments of creep deformation are approximately logarithmically decreasing in time. The difference in the evaluation of M in different cycles is not large as illustrated in Fig. 6. Therefore, average values of M from all cycles were used in the comparison in Fig. 5.

Final values of M (at 20 mN) are approaching approximately the same level for both “O” and “C” series. It can be supposed that at this stage the material has already undergone a major portion of a short-term creep deformation. These final values are $M_O=28.2\pm 4.4$ GPa for “O” series and $M_C=26.9\pm 1.8$ GPa for “C” series. Assuming Poisson's ratio of cement paste to be 0.2 we can calculate elastic modulus using Eq. (3) as $E_O=27.8$ GPa and $E_C=26.4$ GPa.

The results of M are in good agreement with those found in literature (Table 1). Note that in our case average properties of all hydrated phases were evaluated, e.g. results of M and E are valid for C-S-H and CH compounds as indicated in Table 1.

5.3. Cement Clinker

The matrix of 80 indents was prescribed to the maximum load 10 mN (loading at 0.3 mN/s, 200 s dwelling period and unloading at 0.3 mN/s) as shown in Fig. 7a. Negligible creep behavior was observed during the dwelling period at peak load (Fig. 7b). From that it can be concluded that unhydrated clinkers are not responsible for the time-dependent behavior of cement paste but hydrated products.

Indentation modulus of the indented phase of clinker, i.e. belite (C_2S), was determined as $M=113\pm 11$ GPa. Using the assumption of Poisson's ratio 0.2 leads to the elastic modulus $E=121\pm 14$ GPa (Table 1).

Table 1 – Elastic properties of cement constituents reported in literature and measured by nanoindentation.

Constituent	E(GPa)	Reference
C ₂ S	130±7	Velez et al. [15]
C ₃ S	135±20	Velez et al. [15]
C ₃ A	145±10	Velez et al. [15]
C ₄ AF	125±25	Velez et al. [15]
Alite	125±7	Velez et al. [15]
Belite	127±10	Velez et al. [15]
Belite	121±14	This study
LD-CSH	21.7±2.2	Constantinides and Ulm [4]
HD-CSH	29.4±2.4	Constantinides and Ulm [4]
CH	38±5	Constantinides and Ulm [4]
CSH-CH compound	26.5	Hughes and Trtik [10]
CSH-CH compound	26.4±1.8	This study

Legend: C₂S, C₃S, C₃A, C₄AF, Alite and Belite stand for clinker phases; LD- and HD-CSH stand for low-density and high-density calcium-silicate-hydrates, respectively; CH stands for calcium hydroxide (Portlandite).

5.4. Polymer COC/PE

The COC/PE polymer is definitely more homogeneous on the microscale than the cement paste. It can be treated as a single-phase material within the tested size. Therefore, no selection of indents for COC/PE samples was needed. The total number of indents was more than 50 and only statistical evaluation of all indents was carried out. COC/PE is a soft and ductile material with a similar creep behavior as compared to hydrated cement paste. Analogously to cement paste samples,

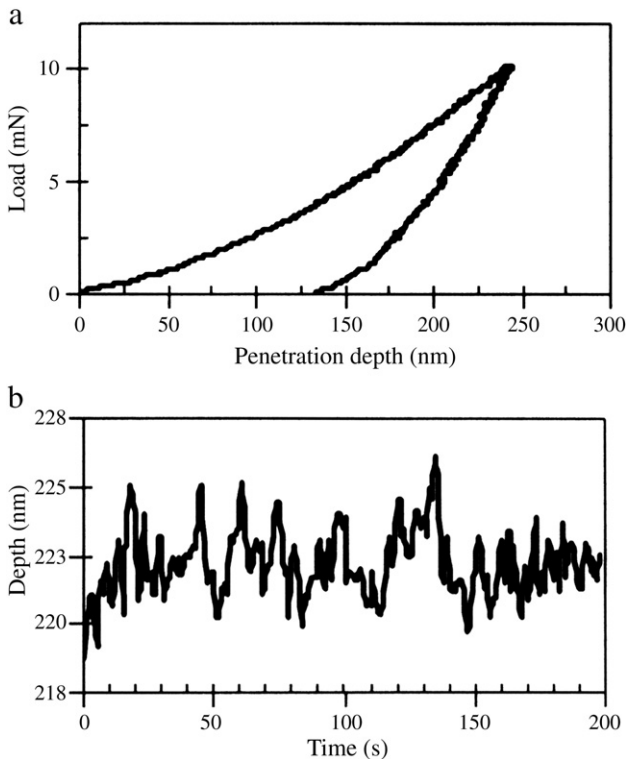


Fig. 7 – (a) Loading diagram of clinker (belite). (b) Evolution of depth deformation during the dwelling period.

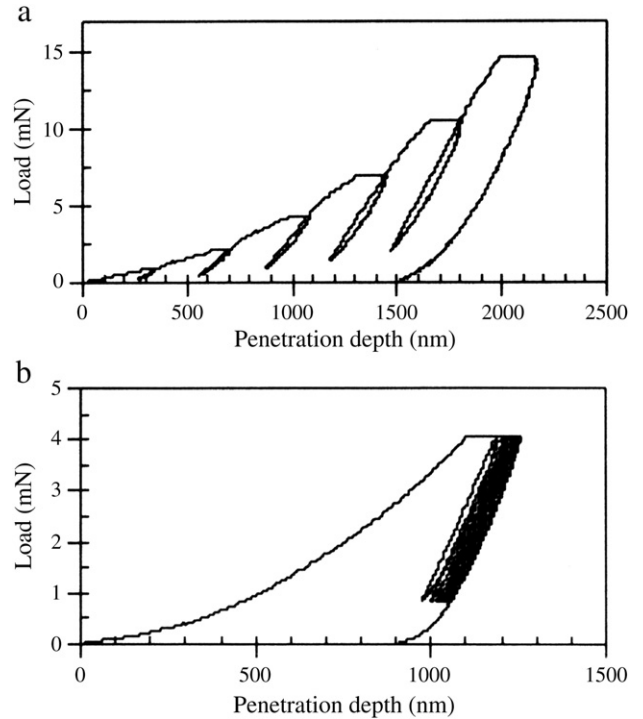


Fig. 8 – Loading diagrams for COC/PE polymer. (a) Multiple loading cycles to increasing load of 1–14.5 mN (“O” series). (b) Cyclic loading to the same load level—4 mN (“C” series). Always a 15 s dwell period at the peak was applied.

two series of tests were carried out. Six loading cycles to increasing peak loads of 1–14.5 mN were applied to “O” series. Ten cycles to the same peak load with a 15 s dwell period were applied to “C” series. Examples of loading diagrams are plotted in Fig. 8. Similarly to cement paste, results on COC/PE exhibit a strong size effect on elastic properties evaluated for “O” series as shown in Fig. 9 where creep plays an important role in the unloading branches of cycles. In contrast, series “C” with cyclic loading to the same load with dwell periods shows a very little size effect in the tested load range for indentation modulus

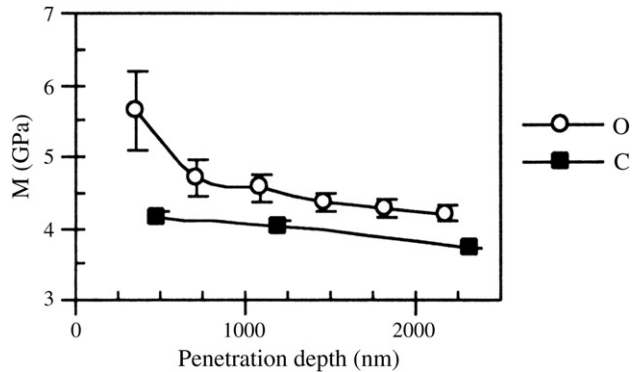


Fig. 9 – Indentation modulus evaluated for the COC/PE polymer. Thin lines represent results for “O” series with increasing loading cycles without a dwell period at the peak, whereas thick lines stand for “C” series tested by cyclic loading to the same load with a 15 s dwell period at the peak.

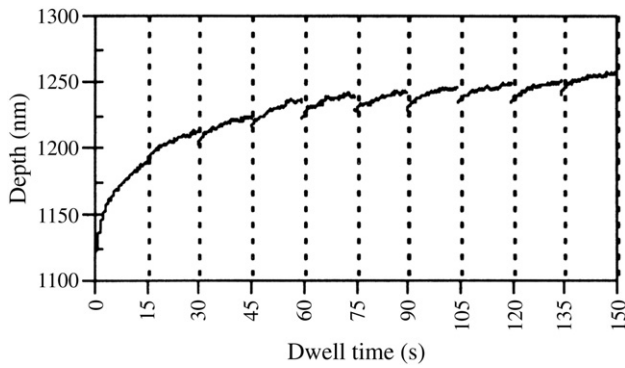


Fig. 10 – Example of the depth increase (creep deformation) during ten dwell periods at cycle peaks (series “C”) on COC/PE for load level of 4 mN. Each column corresponds to one 15 s long cycle. Note that loading and unloading is present between dwell periods (Fig. 7b).

(Fig. 9). Similarly to cement paste, the first loading cycle in the case of “C” series contains a much larger amount of creep deformation than the others as can be seen in Fig. 10.

Generally, results obtained on the COC/PE polymer agree with those obtained for other types of polymers that can be found in literature (e.g. Briscoe et al. [1]). These studies consistently show that the viscoelastic–plastic nature of polymeric materials leads to the above described size effect.

6. Conclusions

An extensive study of creep effects in hydrated cement on the evaluation of elastic properties using nanoindentation was outlined in this paper. It was found that besides the usually considered sources of the indentation size effect the main factor contributing to such interpretations is the experimental loading path and the evolution of creep deformation. It was proved that creep can be accounted for hydrated phases in the cement paste whereas unhydrated clinkers do not exhibit creep behavior at applied loads. A comparison with the COC/PE polymer that shows a similar creeping behavior as hydrated cement was performed.

A strong size effect on elastic properties was observed for cement paste loaded in increasing load cycles with no dwell period at peaks. Rounding of the loading diagram on the unloading branch indicates the influence on creep deformations and consecutively on the evaluation of elastic properties. In contrast, cyclic loading to the same load together with long dwell periods leads to minimizing such spurious size effect, both for cement paste and the COC/PE polymer. Generally, creep deformation of the material is decreasing approximately logarithmically with time. The first dwelling period in the case of cycling to the same peak load contains the majority of the creep deformation whereas the second and successive loading cycles contain less creep deformation. From this study it can

be concluded that long dwelling periods together with cyclic loading to the same peak load should be applied for a proper assessment of elastic properties of materials like cement paste or polymers showing significant time-dependent behavior.

ACKNOWLEDGEMENT

The support of the Ministry of Education of the Czech Republic (project MSM 6840770003) is gratefully acknowledged.

REFERENCES

- [1] Briscoe BJ, et al. Nano-indentation of polymeric surfaces. *J Appl Phys* 1998;31:2395–405.
- [2] Choi Y, Van Vliet KJ, Li J, Suresh S. Size effect on the onset of plastic deformation during nanoindentation of thin films and patterned lines. *J Appl Phys* 2003;94(9).
- [3] Constantinides G, Ulm FJ, Van Vliet K. On the use of nanoindentation for cementitious materials. *Mat Struct* 2003;36:191–6.
- [4] Constantinides G, Ulm FJ. The effect of two types of C-S-H on the elasticity of cement-based materials: results from nanoindentation and micromechanical modeling. *Cem Concr Res* 2004;34(1):67–80.
- [5] Detwiler RJ, et al. Preparing specimens for microscopy. *Concr Int* 2001;23(11).
- [6] Doerner MF, Nix WD. A method for interpreting the data from depth-sensing indentation instruments. *J Mater Res* 1986; 1(4):601–9.
- [7] Elmustafa AA, Stone DS. Indentation size effect in polycrystalline F.C.C. metals. *Acta Mater* 2002;50(14):3641–50.
- [8] Fischer-Cripps AC. Nanoindentation. Springer; 2002.
- [9] Grunlan JC, et al. Preparation and evaluation of tungsten tips relative to diamond for nanoindentation of soft materials. *Rev Sci Instrum* 2001;72(6):2804–10.
- [10] Hughes JJ, Trtik P. Micro-mechanical properties of cement paste measured by depth-sensing nanoindentation: a preliminary correlation of physical properties with phase type. *Mater Charact* 2004;53:223–31.
- [11] ISO 4287-1997. Geometrical product specifications (GPS)—surface texture: profile method—terms, Definitions and surface texture parameters.
- [12] Li H, Ghosh A, Yan YH, Bradt RC. The frictional component of the indentation size effect in low load microhardness testing. *J Mater Res* 1993;8(5):1028–32.
- [13] Nix WD, Gao H. Indentation size effects in crystalline materials: a law for strain gradient plasticity. *J Mech Phys Solids* 1998;46(3):411–25.
- [14] Oliver WC, Pharr GM. An improved technique for determining hardness and elastic modulus using load and displacement sensing indentation experiments. *J Mater Res* 1992;7:1564–83.
- [15] Velez K, et al. Determination of nanoindentation of elastic modulus and hardness of pure constituents of Portland cement clinker. *Cem Concr Res* 2001;31:555–61.
- [16] Wei Y, Wang X, Zhao M. Size effect measurement and characterization in nanoindentation test. *J Mater Res* 2004;19 (1):208–17.